Synthesis, Crystal Structure, and Magnetic Properties of a Three-Dimensional Hydroxide Sulfate: $Mn_5(OH)_8SO_4$

Yong Fan,[a] Guang Hua Li,[a] Lei Yang,[a] Zhi Ming Zhang,[a] Yan Chen,[a] Tian You Song,*[a] and Shou Hua Feng*[a]

Keywords: Hydroxy sulfate / Hydrothermal synthesis / Magnetic properties / Thermodiffractometry / Structure elucidation

A 3D hydroxysulfate, $Mn_5(OH)_8SO_4$, formed from a mild hydrothermal reaction has been reported. The compound crystallizes in the triclinic system $P\bar{1}$ with cell parameters a = 7.5501(5) Å, b = 8.5558(6) Å, c = 8.6059(5) Å, α = 98.122(4)°, β = 102.370(4)°, γ = 99.646(4)°, V = 526.19(6) Å^3 and Z = 2. The crystal structure consists of a 3D framework with channels along the c-axis. In this structure, the manganese atoms in the distorted pentahedra and octahedra are interconnected by OH groups to form layers along the bc plane. These layers are further connected with MnO_5 distorted pentahedra, MnO_6 octahedra and $[SO4]^{2-}$ tetrahedra, resulting in a complicated network. The temperature dependence of the magnetic susceptibility shows a weak antiferromagnetic interaction in the compound.

Introduction

Recently, there has been growing interest in the study of structurally and chemically diverse microporous materials, especially those containing transition elements, because they have potential applications as ion exchangers, catalysts, and advanced materials with novel magnetic and electronic properties.[1–8] The discovery of structures with novel topologies and properties is dependent upon creative synthesis from combinations of tetrahedral anions and polyhedrally coordinated transition metal cations.[9–13] In these materials, anions such as phosphates, germanates, and arsenates are often involved as $[TO_4]$ units (T = tetrahedrally coordinated elements) of inorganic frameworks. Frameworks containing sulfate anions have been considerably less investigated, which is surprising since sulfates are known to promote a wide range of structural arrangements in inorganic solids.[14] From the synthetic chemistry point of view, transition-metal sulfates are very difficult to obtain as single crystals by hydrothermal techniques.

Since the pioneering works of Rao et al. some hybrid porous sulfates and inorganic sulfates containing transition elements have been reported. Wang et al. reported a double-chain copper sulfate.[15] Paul et al. recently reported several Kagomé lattices and other types of layered iron and cobalt sulfates.[16–20] S. Vilminot et al. reported a layered cobalt sulfate.[21] M. J. Rosseinsky et al. have also reported several layered cobalt sulfates.[22,23] M. I. Khan et al. reported a layered vanadium sulfate.[24] In most of the previous compounds prepared by hydrothermal techniques, the layers were like modified brucite, having some of the $[MO_6]$ (M = octahedrally coordinated metal element) octahedra replaced by $[TO_4]$ tetrahedra above and below the vacancies, whereas now a truly brucite-type magnetic layered compound has been reported by S. Vilminot et al.[25] There are much fewer 3D compounds reported. Wright et al. reported a 3D scandium sulfate.[26] C. N. R. Rao et al. have reported a 3D nickel sulfate.[27] S Vilminot et al. reported another nickel sulfate.[28] O. Hare et al. have synthesized several uranium sulfates, one of which has a 3D structure.[29–31] Metal sulfates without entrained organic cations also exhibit interesting catalytic, ion-exchange, and magnetic properties, and they have higher thermal stability relative to metal sulfate hybrids.

There is only one manganese sulfate compound, reported by S. Vilminot et al[32], which has a layered structure. Here we report the synthesis and structure of a 3D manganese sulfate, $Mn_5(OH)_8SO_4$, which has the highest metal/sulfur ratio yet reported. It is another member of the well-known basic transition-metal sulfate family.[33–37] The magnetic properties of this compound are also reported. A thermodiffractometric study reveals that the compound has a high thermal stability.

Results and Discussion

Characterization

The ICP analysis of the product shows the wt.-% of Mn and S to be 54.11 and 6.18, respectively, indicating a Mn/S

[a] State Key Laboratory of Inorganic Synthesis and Preparative Chemistry, College of Chemistry, Jilin University, Changchun 130012, P. R. China
Fax: +86-431-5168624
E-mail: shfeng@mail.jlu.edu.cn
Supporting information for this article is available on the WWW under http://www.eurjic.org or from the author.

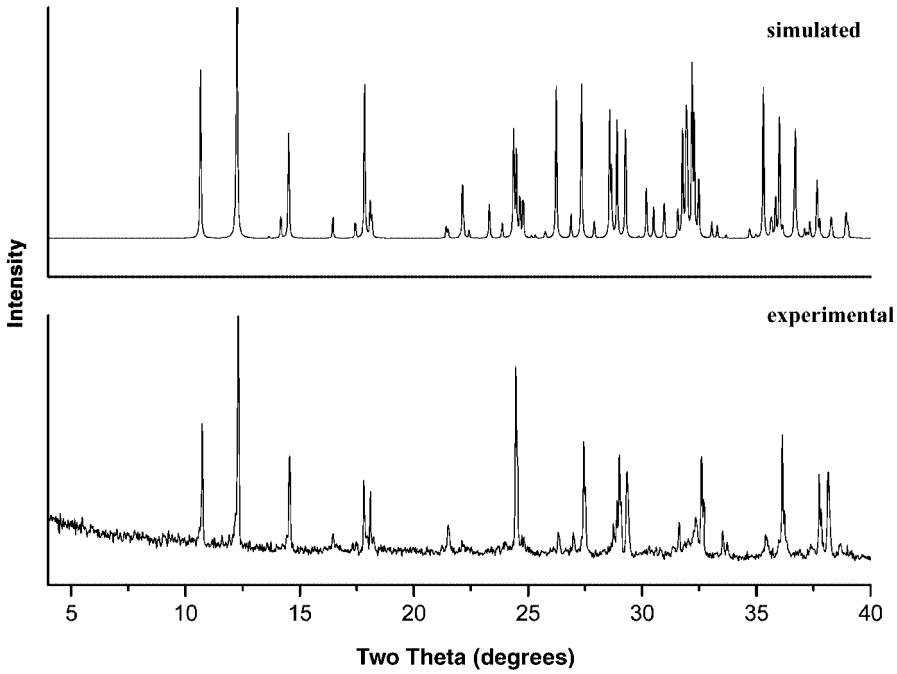

Figure 1. Experimental and simulated powder X-ray diffraction patterns for **1**.

ratio of 5:1, which is in agreement with the experimental wt.-% values of 54.26 and 6.36 based on the ideal formula given by single-crystal X-ray diffraction analysis.

The powder X-ray diffraction pattern was consistent with the simulated one as shown in Figure 1. The positions of the diffraction peaks in both patterns correspond well, which indicates the phase purity of the as-synthesized sample. The difference in reflection intensities between the simulated and experimental patterns was due to the variation in the crystal orientation of the powder sample.

An IR spectrum was recorded between 4000 and 400 cm^{-1} (Figure S2, Supporting Information; for Supporting Information see also the footnote on the first page of this article). The series of sharp bands in the 3635–3430-cm^{-1} and the 850–650-cm^{-1} regions are attributed to O–H. The typical vibrational bands of SO_4^{2-} are observed in the 1150–590-cm^{-1} range. The ν_3 and ν_4 vibrational bands of the sulfate group appear at 1150–1045 cm^{-1} and 650–590 cm^{-1}, respectively. The bands centered at 916 cm^{-1} are attributed to ν_1 vibrational bands of the sulfate group. The bands centered at 470 cm^{-1} and 425 cm^{-1} are attributed to O–Mn vibrations.

The combined thermogravimetric analysis-differential thermal analysis (TGA-DTA) of $Mn_5(OH)_8SO_4$ was carried out in air from room temperature to 900 °C by using a heating rate of 10 °C·min^{-1} and is shown in Figure 2. The results show three mass losses, two sharp and one broad. The first mass loss of about 10.9%, occurring in the region 198–362 °C, with a strong endotherm centered at 299 °C, corresponds to the loss of three H_2O groups (calcd. 10.7%) from six OH groups. The second mass loss of 3.9%, in the region 362–571 °C, corresponds to the loss of one H_2O from two OH groups (calcd. 3.6%). Two weak exotherms, centered at 336 °C and 381 °C, indicate structural changes. After that there is a slight weight gain starting at 571 °C, three weak exotherms centered at 542 °C, 597 °C, and 647 °C, indicating that some of the Mn^{II} ions have been oxidized. However, it is difficult to determine this weight gain accurately, as this process overlaps slightly with the weight loss due to the decomposition of the SO_4^{2-} fraction. Decomposition of

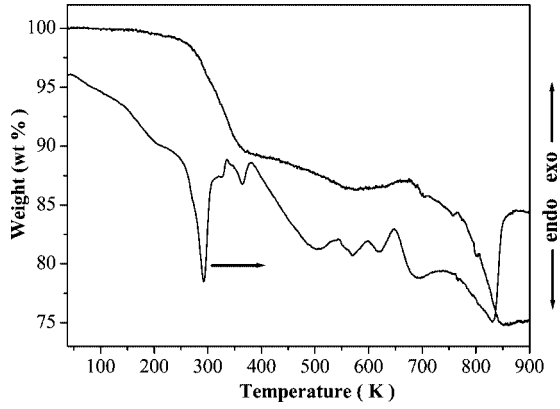

Figure 2. TGA-DTA curves for **1**.

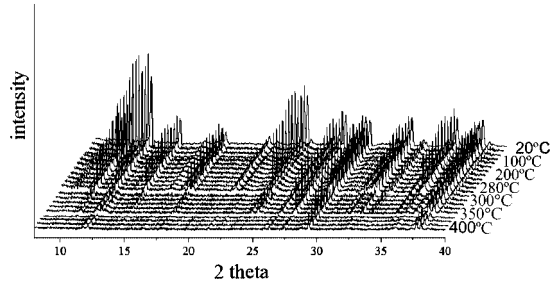

Figure 3. X-ray thermodiffractometric pattern for **1**.

the SO_4^{2-} fraction starts to take place at 830 °C as a strong exothermic effect. The TG curve shows a continuous weight loss in this region. The final thermal decomposition product is Mn_2O_3 with its standard powder diffraction pattern (PDF database No: 41–1442).

A thermodiffractometric study of **1** (Figure 3) was undertaken to characterize the water loss. Compound **1** is only stable up to 280 °C; above this temperature water is lost.

Description of Structure

The asymmetric unit of **1** contains 29 non-hydrogen atoms (5 Mn, 1 S, and 23 O atoms) as shown in Figure 4. The Mn atoms adopt three different types of coordination: pentahedral, distorted pentahedral, and distorted octahedral, which is more complex than other basic sulfates.[33–37] In other metal sulfates, the metal atoms adopt only one octahedral or tetrahedral coordination, only $Zn(OH)_2$·$ZnSO_4$ adopts octahedral and tetrahedral coordination. Mn(1) is coordinated to five oxygen atoms [O(1), O(2), O(2A), O(3), and O(4)] from five different OH groups and shows as a slightly distorted pentahedron. O(2), O(2A), O(3), and O(4) form a plane with O(1) occupying the axial position. The Mn atom is slightly above or below the plane of the pyramid. The Mn(1)–O bond lengths range from 2.151(3) to 2.168(3) Å. Mn(2), Mn(3), and Mn(5) all adopt octahedral coordination: Mn(2) and Mn(3) are coordinated to six oxygen atoms from five different OH groups and a sulfate group, Mn(5) is coordinated to six oxygen atoms from four different OH groups and two different sulfate groups, with typical geometrical parameters {d_{av}[Mn(2)–O] = 2.211(3) Å, d_{av}[Mn(3)–O] = 2.217(3) Å, and d_{av}[Mn(5)–O] = 2.239(3) Å}. Mn(4) is coordinated by five oxygen atoms from five different OH groups; O(6A), O(8), and O(9A) form a distorted plane, whereas O(1) and O(9) occupy the axial positions, forming a distorted pentahedron. It is worth noting that the bond lengths of Mn(1)–Mn(3), Mn(1)–Mn(2), and Mn(2)–Mn(2)$^{\#2}$ are 3.1639(10) Å, 3.1729(9) Å, and 3.0933(14) Å, respectively.

The sulfate group in each asymmetric unit is tetrahedrally coordinated through its two oxygen atoms, O(10) and O(11A), and bonded to two different Mn atoms, Mn(2) and Mn(3), through the μ_3-O(7) bridge. O(12), the shortest of the S–O bonds, is a terminal oxygen with d_{av}(S–O) = 1.469(4) Å.

Formation of the 3D structure (Figure 5) can be explained by the linking of layers (Figure 6) through columns (Figure 7), which form empty channels. Each layer is obtained by linking chains of Mn atoms, bridged by O atoms. There is no similarity to the well-known structures of most basic hydroxide sulfates of divalent metals in which there are 1D chains or 2D layers linked by hydrogen bonding to form more complex networks. Mn(1)O(5), Mn(2)O(6), and Mn(3)O(6) form a chain (Chain 1), and Mn(1A)O(5), Mn(2A)O(6), and Mn(3A)O(6) form a neighboring chain (Chain 2). In Chain 1, Mn(1) is bridged to Mn(2) through 2 O atoms [O(1) and O(2)] on one side and to Mn(3) through 2 O atoms [O(3) and O(4)] on the other side. The fifth O atam [O(2A)] bridges Mn(2) to Mn(1A) and Mn(2A) of Chain 2. Mn(2) is further bridged to Mn(3) through two O atoms [O(6) and O(7)]. O(2) bridges Chain 1 to the Mn(1A) of Chain 2. O(5) and O(5A) bridge Mn(2) to Mn(2A) of Chain 2′, which faces the opposite direction to that of Chain 2. O(1) bridges Mn(1), Mn(2), and Mn(4)

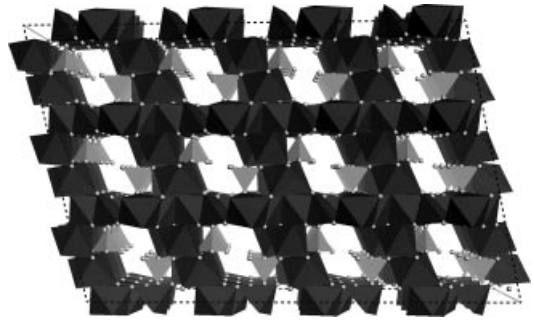

Figure 5. View of the crystal structure of the complex along the *c*-axis. SO_4^{2-} tetrahedra are gray and MnO_x polyhedra are black.

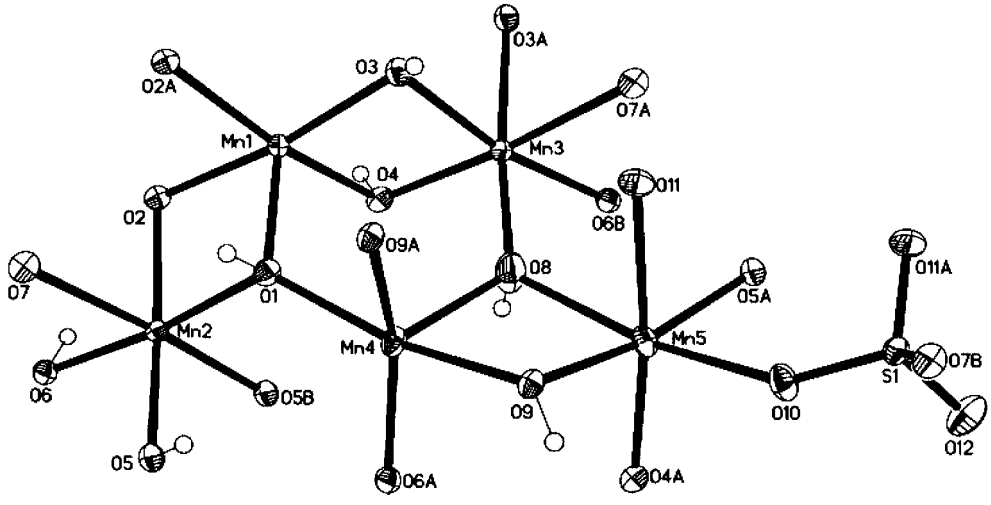

Figure 4. ORTEP drawing of the asymmetric unit of **1** showing the atom-labeling scheme (50% thermal ellipsoids).

of the column which lie perpendicular to the layer of the chains. Mn(3) is bridged to Mn(1) and Mn(2) in the same type of chain as explained earlier for Mn(1) and Mn(2) using four of its coordination sites. Its fifth coordinating oxygen, O(8), bridges it to Mn(4) and Mn(5) of the column, which runs out of the layer, and the sixth oxygen, O(3), bridges it to Mn(1A) and Mn(3A) of Chain 2. Thus the two neighboring chains run parallel but in opposite directions to each other. They are linked together through bridging O atoms to form a complex layer (Figure 6).

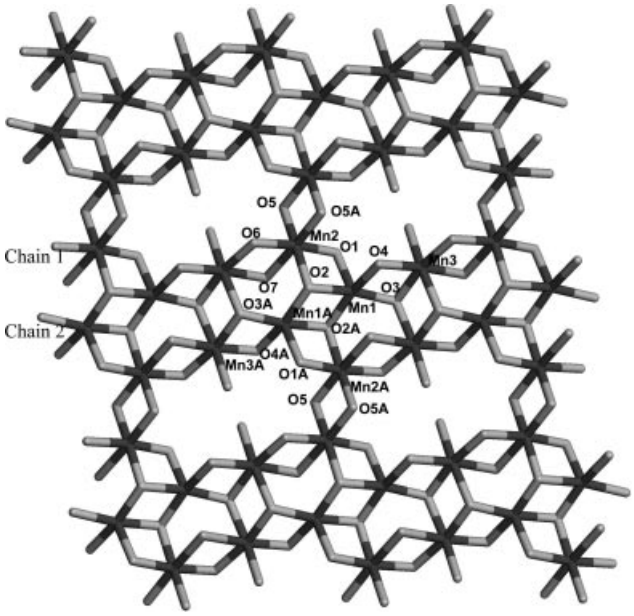

Figure 6. View of the structure perpendicular to the plane of the Mn/O/H layer orientated in the [100] plane.

Between the layers are complex columns formed by $Mn(5)O_6$ octahedra, $Mn(4)O_5$ distorted pentahedra and sulfate tetrahedra. In each column, two $Mn(5)O_6$ octahedra, two $Mn(4)O_5$ distorted pentahedra, and two sulfates are tetrahedrally linked together through edge or corner sharing to form a unit. These units are linked to form the infinite column (Figure 7).

The 3D structure is obtained by linking the layers in a unique pattern. The consecutive layers are linked to each other through complex columns which are perpendicular to them and thus form empty channels that can be viewed along the *c*-axis (Figure 5).

Magnetic Susceptibility

The temperature dependence of magnetic susceptibility at 5000 Oe was measured for **1** in the range 4–300 K (Figure 8). The experimental data were fitted by using the Curie–Weiss equation $\chi_m = C_m/(T - \Theta)$. The Curie constant is 21.72 emu·K·mol^{-1}. The Weiss constant, Θ, was determined to be –134.35 K in the temperature range of 25 K to 300 K, which suggests rather strong antiferromagnetic interactions between neighboring Mn atoms. This behavior is fully confirmed by the onset of a net maximum in the χ_m vs. T curve at 8.3 K; this maximum can be ascribed to the Neel temperature. The effective magnetic moment at 300 K, calculated from $\mu_{eff} = (8\chi_m T/5)^{1/2}$, is 5.64 μ_B per Mn, which is slightly lower than the theoretically expected value of 5.92 μ_B for Mn^{2+} in a high-spin d^5 system. This may be caused by the interaction of Mn atoms.

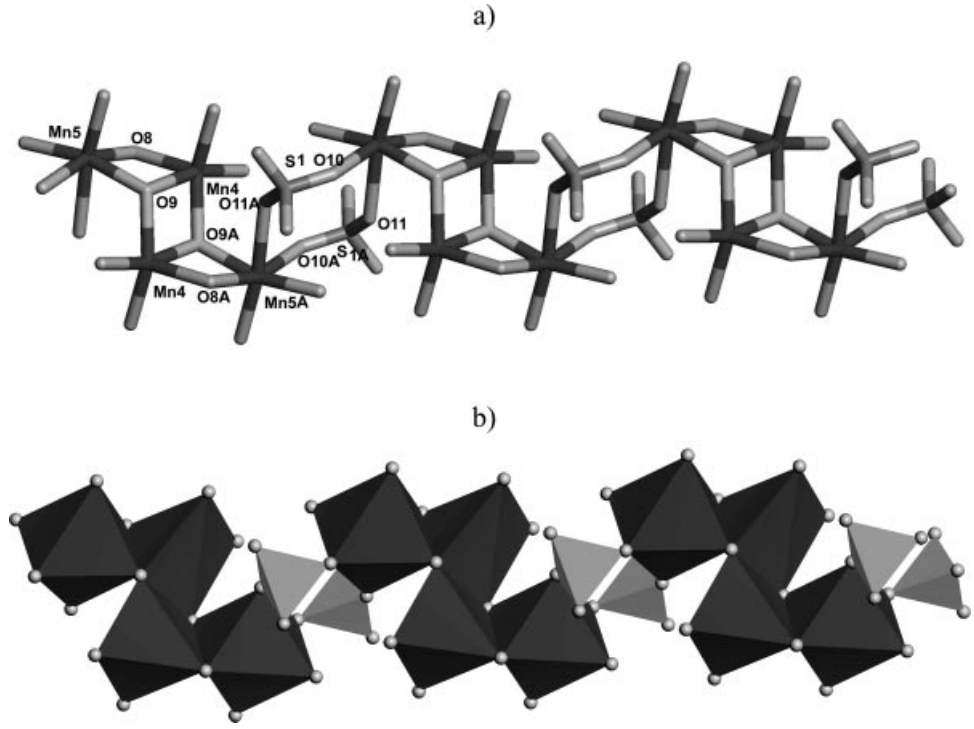

Figure 7. Complex column formed by $Mn(5)O_6$ octahedra, $Mn(4)O_5$ distorted pentahedra and sulfate tetrahedra.

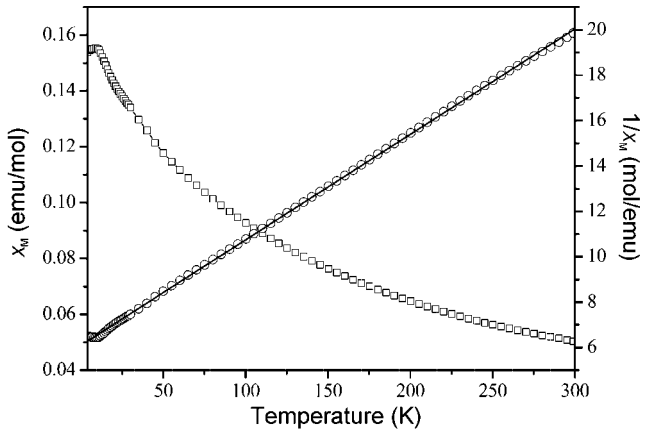

Figure 8. Thermal evolution of χ_m (□), linear curve (-) and $1/\chi_m$ (O) curves of **1**.

Conclusions

A 3D compound, $Mn_5(OH)_8SO_4$, has been synthesized hydrothermally from Mn^{II} ions and H_2SO_4. It has been structurally characterized by single-crystal X-ray diffraction analysis. The phase purity of the product has been confirmed by powder X-ray diffraction. The structure consists of alternately connected $\{MnO_x\}$ and $\{SO_4\}$ units which form a complex network. This compound is stable below 280 °C. The temperature dependence of the magnetic susceptibility shows a rather strong antiferromagnetic interaction in the compound.

Experimental Section

Characterization: The product was prepared by a hydrothermal method. In a typical synthesis, $MnCl_2{\cdot}4H_2O$ (0.199 g) was dissolved in water (10 mL) with stirring, and H_2SO_4 (0.1 mL) was added to form a solution. Cyclohexyl amine (2.4 mL) was added to this solution with continuous stirring until a homogeneous reaction mixture was formed. The final mixture with a molar ratio of $MnCl_2{\cdot}4H_2O/H_2SO_4$/cyclohexyl amine of 1:5:20 was crystallized in a 23-mL PTFE-lined acid digestion bomb at 170 °C for 5 d. The resultant product of pink sticks was filtered and washed thoroughly with distilled water. The yield was 25% based on Mn. Inductively coupled plasma (ICP) analysis was performed with a Perkin–Elmer Optima 3300DV ICP instrument. X-ray powder diffraction (XRD) data were collected with a Siemens D5005 diffractometer with Cu-K_α radiation (λ = 1.5418 Å). The step size was 0.02°, and the count time was 4 s. The infrared (IR) spectrum was recorded within the 400–4000 cm^{-1} region on a Nicolet Impact 410 FTIR spectrometer using KBr pellets. A Perkin–Elmer DTA 1700 was used to obtain the differential thermal analysis (DTA) and a Perkin–Elmer TGA 7 to obtain thermogravimetric analysis (TGA) curves in an air with a heating rate of 10 °C·min^{-1}. X-ray thermodiffractometry was performed in the furnace of a Siemens D-5000 diffractometer in the θ-θ mode in air. Magnetic susceptibility data were collected on the basis of a 0.0227 g sample over the temperature range of 4–300 K at a magnetic field of 5 kG with a Quantum Design MPMS-7 SQUID magnetometer.

X-ray Crystallographic Study: A suitable pink single crystal with dimensions $0.35\times0.32\times0.30$ mm^3 was glued to a thin glass fiber and mounted on a Siemens Smart CCD diffractometer equipped with a normal-focus, 2.4-kW sealed-tube X-ray source (graphite-monochromatic Mo-K_α radiation (λ = 0.71073 Å). Intensity data were collected at a temperature of 293 ± 2 K. Data processing was accomplished with the SAINT processing program.[38] The total number of measured reflections and observed unique reflections were 2885 and 1822, respectively. Intensity data of 1822 independent reflections ($-7 \le h \le 8$, $-10 \le k \le 7$, $-10 \le l \le 10$) were collected in the ω scan mode. An empirical absorption correction was applied using the SADABS program with T_{max} = 0.4000 and T_{min} = 0.3001). The structure was solved in the space group $P\bar{1}$ by direct methods and refined on F^2 by full-matrix least-squares using SHELXTL97.[39] The sulfur and manganese atoms were located first. Oxygen was then found in the difference Fourier map. The hydrogen atoms were placed geometrically. All non-hydrogen atoms were refined with anisotropic thermal parameters. The compound crystallizes in the triclinic system $P\bar{1}$ with cell parameters a = 7.5501(5) Å, b = 8.5558(6) Å, c = 8.6059(5) Å, α = 98.122(4)°, β = 102.370(4)°, γ = 99.646(4)°, V = 526.19(6) $Å^3$ and Z = 2. A summary of the crystallographic data is presented in Table 1. Further details of the crystal-structure investigation(s) may be obtained from the Fachinformationszentrum Karlsruhe, 76344 Eggenstein-Leopoldshafen, Germany, on quoting the depository number CSD-391307 (Crysdata@FIZ-Karlsruhe.de).

Table 1. Crystal data for title compound **1**.[a]

Empirical formula	$H_8Mn_5O_{12}S$
Formula weight	506.82
Temperature	293(2) K
Wavelength	0.71073 Å
Crystal system	Triclinic
Space group	$P\bar{1}$
Unit cell dimensions	a = 7.5501(5) Å
	b = 8.5558(6) Å
	c = 8.6059(5) Å
	α = 98.122(4)°
	β = 102.370(4)°
	γ = 99.646(4)°
Volume	526.19(6) $Å^3$
Z	2
Calculated density	3.199 m^3
Absorption coefficient	6.092
F(000)	490
Crystal size	$0.35\times0.32\times0.30$ mm
Reflections collected/unique	2885/1822 [R_{int} = 0.0365]
Data/restraints/parameter	1822/4/193
Goodness-of-fit on F^2	1.071
Final R indices [$I > 2\sigma(I)$]*	R_1 = 0.0366, wR_2 = 0.0868

[a] $R_1 = \Sigma||F_o|-|F_c||/\Sigma|F_o|$; $wR_2 = \{\Sigma[w(F_o^2-F_c^2)^2]/\Sigma[w(F_o^2)]^2\}^{1/2}$.

Acknowledgments

We thank the National Natural Science Foundation of China (Grant No. 20071013 and 20301007) and the State Basic Research Project of China (Grant G2000077507).

[1] T. Pinnavaia, *Science* **1983**, *220*, 365–371.
[2] T. Shichi, K. Takagi, Y. Sawaki, *Chem. Commun.* **1996**, 2027–2028.
[3] J. M. Thomas, *Angew. Chem.* **1994**, *106*, 963–989.
[4] M. E. Davis, *Chem. Eur. J.* **1997**, *3*, 1745–1750.
[5] T. Bein, *Chem. Mater.* **1996**, *8*, 1636–1653.
[6] D. W. Lewis, D. J. Willock, C. R. A. Catlow, J. M. Thomas, G. J. Hutchings, *Nature* **1996**, *382*, 604–606.
[7] S. P. Newman, W. Jones, *New J. Chem.* **1998**, *22*, 105–115.

[8] K. Cheetham, G. Férey, T. Loiseau, *Angew. Chem. Int. Ed.* **1999**, *38*, 3269–3292.
[9] I. Bull, P. S. Wheatley, P. Lightfoot, R. E. Morris, E. Sastre, A. Wright, *Chem. Commun.* **2002**, 1180–1181.
[10] J. Rocha, M. W. Anderson, *Eur. J. Inorg. Chem.* **2000**, *5*, 801–818.
[11] J. Rocha, P. Ferreira, Z. Lin, P. Brandao, A. Ferreira, J. D. P. de Jesus, *J. Phys. Chem. B* **1998**, *102*, 4739–4744.
[12] J. Rocha, P. Ferreira, L. D. Carlos, A. Ferreira, *Angew. Chem. Int. Ed.* **2000**, *39*, 3276–3279.
[13] D. Ananias, A. Ferreira, J. Rocha, P. Ferreira, J. P. Rainho, C. Morais, L. D. Carlos, *J. Am. Chem. Soc.* **2001**, *123*, 5735–5742.
[14] M. S. Wickleder, *Chem. Rev.* **2002**, *102*, 2011–2087.
[15] L. Xu, E. B. Wang, J. Peng, R. D. Huang, *Inorg. Chem. Commun.* **2003**, *6*, 740–743.
[16] C. N. R. Rao, E. V. Sampathkumaran, R. Nagarajan, G. Paul, J. N. Behera, A. Choudhury, *Chem. Mater.* **2004**, *16*, 1441–1446.
[17] G. Paul, A. Choudhury, E. V. Sampathkumaran, C. N. R. Rao, *Angew. Chem. Int. Ed.* **2002**, *41*, 4297–4300.
[18] G. Paul, A. Choudhury, C. N. R. Rao, *Chem. Commun.* **2002**, 1904–1905.
[19] G. Paul, A. Choudhury, C. N. R. Rao, *Chem. Mater.* **2003**, *15*, 1174–1180.
[20] J. N. Behera, G. Paul, A. Choudhury, C. N. R. Rao, *Chem. Commun.* **2004**, 456–457.
[21] M. B. Salah, S. Vilminot, M. R. Plouet, G. Andre, T. Mhirid, M. Kurmoo, *Chem. Commun.* **2004**, 2548–2549.
[22] A. Rujiwatra, C. J. Kepert, M. J. Rosseinsky, *Chem. Commun.* **1999**, 2307–2308.
[23] A. Rujiwatra, C. J. Kepert, J. B. Claridge, M. J. Rosseinsky, H. Kumagai, M. Kurmoo, *J. Am. Chem. Soc.* **2001**, *123*, 10584–10594.
[24] M. I. Khan, S. Cevik, R. J. Doedens, *Inorg. Chim. Acta* **1999**, *292*, 112–116.
[25] M. B. Salah, S. Vilminot, M. Richard-Plouet, G. Andre, T. Mhiri, M. Kurmoo, *Chem. Commun.* **2004**, 2548–2549.
[26] I. Bull, P. S. Wheatley, P. L. Russe, E. Morris, E. Sastre, P. A. Wright, *Chem. Commun.* **2002**, 1180–1181.
[27] N. Behera, K. V. Gopalkrishnan, C. N. R. Rao, *Inorg. Chem.* **2004**, *43*, 2636–2642.
[28] S. Vilminot, M. R. Plouet, G. Andre, D. Swierczynski, F. B. Vigneron, M. Kurmoo, *Inorganic Chemistry* **2003**, *42*, 6859–6967.
[29] M. Doran, A. J. Norquist, D. O'Hare, *Chem. Commun.* **2002**, 2946–2947.
[30] J. Norquist, P. M. Thomas, M. Doran, D. O'Hare, *Chem. Mater.* **2002**, *14*, 5179–5184.
[31] P. M. Thomas, A. J. Norquist, M. B. Doran, D. O'Hare, *J. Mater. Chem.* **2003**, *13*, 88–92.
[32] M. B. Salah, S. Vilminot, T. Mhiri, M. Kurmoo, *Eur. J. Inorg. Chem.* **2004**, 2272–2276.
[33] V. Y. Ittaka, H. R. Oswald, S. Locchi, *Acta Crystallogr.* **1962**, *15*, 559.
[34] V. K. Mereiter, *Acta Crystallogr. Sect. B* **1979**, *35*, 579–585.
[35] M. Gentsch, K. Weber, *Acta Crystallogr. Sect. C* **1984**, *40*, 1309–1311.
[36] I. J. Bear, I. E. Grey, I. C. Madsen, I. E. Newnham, L. J. Rogers, *Acta Crystallogr. Sect. B* **1986**, *42*, 32–39.
[37] E. Dubler, H. R. Oswald, *Die Kristallstruktur von Trikobalt(II)-dihydrodisulfat-dihydrat, $Co_3(OH)_2(SO_4)_2{\cdot}2H_2O$*, Teil der Dissertation von E. Dubler, University of Zürich, **1970**.
[38] Software Packages SMART and SAINT, Siemens AnalyticalX-ray Instruments, Inc., Madison, WI, **1996**.
[39] SHELXTL, version 5.1; Siemens Industrial Automation, Inc, Madison, WI, **1997**.

Received: February 3, 2005
Published Online: July 7, 2005

